

Original Article

Nature Inspired Optimization with Hybrid Machine Learning Model for Cardiovascular Disease Detection and Classification

S. Sivasubramaniam¹, S. P. Balamurugan²

¹Department of Computer and Information Science, Annamalai University.

²Programmer, Department of Computer and Information Science, Annamalai University.

¹Corresponding Author: sivaresearchscholarau@gmail.com

Received: 16 August 2022

Revised: 13 November 2022

Accepted: 25 November 2022

Published: 24 December 2022

Abstract - Cardiovascular disease can be considered a lethal disease which affects people all over the globe. Accurate and prompt heart disease prediction can assist physicians in decision-making. Therefore, machine learning (ML) models can be applied to examine medical data for the data classification process. Since the medical dataset comprises repetitive and unwanted features affecting the classification performance, feature selection (FS) techniques can be employed. Recently, several works have applied metaheuristic algorithms for the FS process. This study presents a new mayfly optimization-based FS with a hybrid ML (MFOFS-HML) model for heart disease detection and classification. The presented MFOFS-HML model applies data pre-processing to convert the actual data into a useful format. In addition, the MFOFS technique is used for the effective selection of features from the pre-processed data. Finally, the hybrid convolutional neural network (CNN) with Hopfield neural network (HNN) hybrid (CNN-HNN) mechanism is employed for the detection and classification process. The CNN-HNN model involves the inclusion of the HNN model at the end of the CNN layer, which helps improve the classification performance with the MFO-FS technique showing the novelty of the work. The experimental validation of the MFOFS-HML model is tested under two benchmark datasets, Cleveland and Framingham datasets. A brief comparison study reported the enhanced outcomes of the presented MFOFS-HML algorithm over recent methods.

Keywords - Heart disease prediction, Machine learning, Hybrid model, Feature selection, Metaheuristics.

1. Introduction

With the improvement of the information era, the computer-aided system generates an enormous amount of raw information, increasing the new center of power. Obtaining considerable knowledge from this information is challenging for the practitioner [1]. Data mining (DM), deep learning (DL), Artificial Intelligence (AI), and machine learning (ML) are promising and relatively modern technologies to obtain relationships or identify important databases using statistical methods. Medical DM and knowledge exploration constitute a comparatively modern and emerging domain of great interest to many research workers [2, 3]. With the development of medical dataset collection, the physician has the capacity to better identify diseases [4]. Furthermore, computation biomedical systems can achieve greater prediction accuracy and accelerate decision-making in various diseases like kidney diseases, heart diseases, skin diseases, cancers, and diabetes. Amongst them, cardiovascular disease (CVD) has been recognized as having a high level of mortality in nearly all countries worldwide [26].

World Health Organization (WHO) reported that CVD will raise the mortality rate to nearly thirty million by 2040 [6]. Echocardiogram (heart ultrasound), stress tests (stress ECG, nuclear cardiac, and exercise stress tests), Electrocardiogram (ECG), angiography, and cardiac magnetic resonance imaging (MRI) are the famous test conducted by physicians to assist recognizes CV problems. However, treatment and diagnostic costs are pretty higher for CVD and expensive for the community [7]. As a result, earlier diagnosis of this disease is essential for treatment. In order to attain the status of a CV patient, the hospitals need to gather specific physical values, namely blood sugar, static blood pressure, maximum heart rate, cholesterol, electrocardiogram, and chest pain type.

Nevertheless, manual analysis of heart disease-related datasets is time-consuming and has the disadvantage of misdiagnoses. AI technique is extensively applied in prediction to resolve these problems. Amongst others, DL and ML techniques are predominant [8]. Such prediction methods analyze a considerable number of medical information to define whether a person has the illness and



achieve better prediction results when compared to manual diagnoses.

DM method enables the effective finding of whether the patient is at a high chance of heart disease at earlier stages and, therefore, decreases the cost of treatment and diagnosis [9]. A better classifier solution is needed to be efficient and effective; however, a massive amount of irrelevant and redundant attributes might increase computation costs and the amount of time needed to test and learn multi-label classifiers that reduce classification accuracy.

Feature selection is a powerful mechanism in ML, and DM is increasingly being used in classification models to improve accuracy [10]. Selecting features before using the classification method on the original dataset has several benefits, namely improving classification accuracy, refining the data, and reducing the computational cost. Thus, the FS technique can improve the quality of the classification method. Though several models are available in the literature, it is still needed to enhance heart disease diagnosis classification performance.

This study presents a new mayfly optimization-based FS with a hybrid ML (MFOFS-HML) model for detecting and classifying heart disease. The presented MFOFS-HML model applies data pre-processing to convert the actual data into a useful format. In addition, the MFOFS technique is used for the effective selection of features from the pre-processed data. Finally, the hybrid convolutional neural network (CNN) with Hopfield neural network (HNN) (CNN-HNN) model is employed for the detection and classification process. The experimental validation of the MFOFS-HML algorithm is tested under two benchmark datasets, Cleveland and Framingham datasets.

2. Related Works

In [11], the authors employed the Fast Correlation-Based Feature Selection (FCBF) approach for filtering redundant features to improve the quality of the heart disease classifier. Afterwards, the authors execute a classifier dependent upon distinct classifier techniques, namely Naïve Bayes (NB), Support Vector Machine (SVM), Multilayer Perception (MLP), Random Forest (RF), and K-Nearest Neighbour (KNN) with Artificial Neural Network (ANN) optimizing with Particle Swarm Optimization (PSO) integrated with Ant Colony Optimization (ACO) methods. [12] recommended an ML-based CVD forecast model, which is highly accurate. However, modern ML approaches were used to classify common CVD datasets using Linear Regression, NB, J48, REP Tree, M5P, RT, and JRIP. In [13], the authors have presented a hybrid method for heart disease forecast utilizing RF and SVM. With RF, iterative feature extraction was executed for selecting heart disease features, enhancing the forecast result of SVM for heart disease forecast.

In [27], the authors present a novel multi-modal approach to forecasting CVD based combined on ECG and PCG features. With developing CNNs, the authors extract PCG and ECG deep-coding features correspondingly. The GA has been utilized to screen the integrated feature and attain an optimum feature subset. Afterwards, the authors utilize an SVM for implementing classifiers. In [15], a novel ML technique was presented for predicting heart disease. The presented study utilized the CHD dataset, and data mining approaches like regression and classifiers were utilized. In ML approaches, RF and DT were executed. A new approach to the ML method was designed. During the execution, 3 ML approaches were utilized: RF, DT, and Hybrid model (Hybrid of RF and DT). In [16], the authors establish a classifier method utilizing MLP with Backpropagation (BP) learning technique and FS technique together with biomedical test value for diagnosing heart disease. The clinical analysis was completed commonly by the doctor's knowledge and experience. However, resolved cases were reported of wrong analysis and treatment. The patient has questioned them about taking a count of tests for analysis. In several cases, not every test involves the effectual analysis of diseases.

3. The Proposed Model

This study established a new MFOFS-HML method to detect and classify heart diseases. The proposed MFOFS-HML algorithm involves three major processes: data pre-processing, MFO-FS-based feature subset selection, and CNN-HNN classification. Initially, the presented MFOFS-HML model applies data pre-processing to convert the actual data into a useful format. Followed by the MFOFS technique is used for the effective selection of features from the pre-processed data. At last, the CNN-HNN model is employed for the detection and classification process. Fig. 1 demonstrates the working procedure of the MFOFS-HML approach.

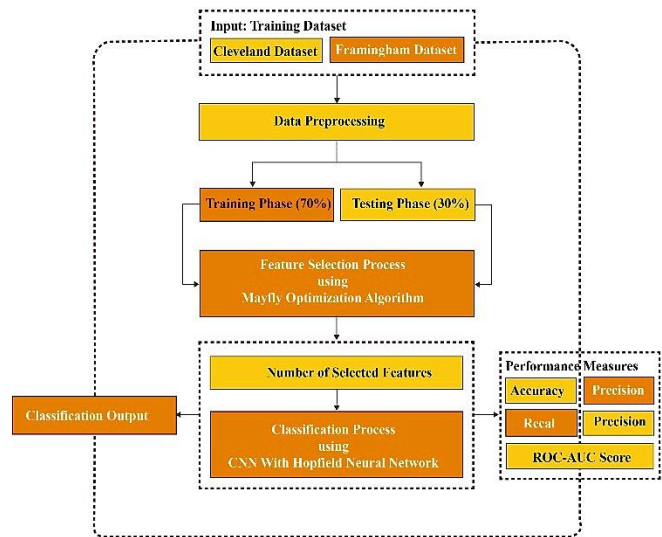


Fig. 1 Working procedure of MFOFS-HML technique

3.1. Data Processing

Initially, the presented MFOFS-HML model applies data pre-processing to convert the actual data into a helpful format. It performs in three stages: data correction, null value removal, and data normalization. Firstly, the incorrect values (such as '?') are filled with null values. Secondly, the null values that exist in the dataset are removed. Thirdly, the min-max data normalization approach is applied to transform the input data into a uniform format. It is commonly utilized to normalize the data into a range of [0, 1] and is represented as follows:

$$x^* = \frac{x - x_{min}}{x_{max} - x_{min}}, \quad (1)$$

Whereas x^* implies the normalization data, x denotes the original information, x_{min} and x_{max} represents the minimal and maximal data values from the existing elements.

3.2. Process involved in MFO-FS Technique

Next to data pre-processing, the MFOFS technique is used for the effective selection of features from the pre-processed data. In the MFO algorithm [17], primarily, two sets of mayflies (MFs) are arbitrarily created, one comprising a female and male population. Assume that all MFs i , during this searching space, arbitrarily defined as a nv -dimensional vector $x^{i,moa}(t) = [x_1^{i,moa}(t), \dots, x_{nv}^{i,moa}(t)]$ and a velocity $v^{i,moa}(t) = [v_1^{i,moa}(t), \dots, v_{nv}^{i,moa}(t)]$. During the iterative procedure, at all the iterations t , the present place of all the MFs is measured by employing an estimation function. In the analysis of the estimation function, at all the iterations t , all the MFs alter their trajectory nearby their personal optimum place, $p_{best}^{i,moa}(t) = [p_{best}^{i,moa}(t), \dots, p_{best}^{i,moa}(t)]$. During the course of the iterative procedure, if an optimum result was initiated, this vector was upgraded. Eventually, at all the iterations, an optimum found place measured by the estimation function saved in $p_{best}^{i,moa}(t)$ was stored from another vector, $g_{best}^{i,moa}(t)$.

3.2.1. Movement of Male Mayflies

Considering that $x^{i,moa}(t)$ implies the existing place of male MF i from the searching space at iteration t , their place was altered by adding a velocity $v_{ml}^i(t+1)$ to present place, based on the following formula:

$$x^{i,moa}(t+1) = x^{i,moa}(t) + v_{ml}^{i,moa}(t+1), \quad (2)$$

Whereas $v_{ml}^{i,moa}(t+1)$ has been provided based on the subsequent formula:

$$v_{ml}^{i,moa}(t+1) = gv_{ml}^{i,moa}(t) + C_1 e^{-\beta r_p^2} co^i(t) + C_2 e^{-\beta r_g^2} so^i(t), \quad (3)$$

In which C_1 and C_2 are denied, g is named the gravity co-efficient and is values defined from the interval of zero and one, but $co^i(t)$ and $so^i(t)$ are addressed correspondingly. At last, β is named the visibility co-efficient and is their value defined empirically, but r_p and r_g are corresponding, the computed Cartesian distance in $x^{i,moa}(t)$ to $p_{best}^i(t)$ and amongst $x^{i,moa}(t)$ and $g_{best}(t)$ based on the subsequent formula:

$$\begin{aligned} & \left\| x^{i,moa}(t) - \bar{x}^{i,moa}(t) \right\| \\ &= \sqrt{\sum_{j=1}^{nv} [x^{ij,moa}(t) - \bar{x}^{ij,moa}(t)]^2} \end{aligned} \quad (4)$$

Whereas $x^{i,moa}(t) = p_{best}^{i,moa}(t)$ or $x^{i,moa}(t) = g_{best}^{i,moa}(t)$. The velocity control, illustrated in Eq. (3), of every MF from the MFO was executed based on the subsequent formula:

$$\begin{aligned} & v_{m1}^{i,moa}(t+1) = \\ & \left\{ \rho_2 v_{m1}^{i,moa}(t) \text{ if } v_{m1}^i(t+1) < \rho_2 v_{m1}^{max}, \text{ if } v_{m1}^{i,moa}(t+1) > v_{m1}^{max}, \right. \\ & \left. v_{m1}^{i,moa}(t+1) \right. \\ &= \begin{cases} v_{m1}^{max}, & \text{if } v_{m1}^{i,moa}(t+1) > v_{m1}^{max}, \\ \rho_2 v_{m1}^{max}, & \text{if } v_{m1}^i(t+1) < \rho_2 v_{m1}^{max}, \end{cases} \end{aligned} \quad (5)$$

Whereas ρ_2 refers to the empirically set arbitrary value, $v_{max} = \rho_1(x_{max} - x_{min})$, whereas x_{max} and x_{min} signifies the upper as well as lower boundaries of the control parameter of devices connected from the power model and ρ_1 has been adjusted in values chosen in the range of zero and one [18].

In order to the step that replicates the nuptial dance, whereas an optimum MFs must continue varying its velocity, the subsequent formula was projected:

$$v_{m1}^{i,moa}(t+1) = v_{m1}^{i,moa}(t) + d \cdot r, \quad (6)$$

In which d represents the co-efficient of nuptial dance and r demonstrates the vector with arbitrary numbers in -1 and 1.

3.2.2. Movement of Female Mayflies

Let us $y^{i,moa}(t)$ implies the present place of female MF i from the searching space, at iteration t , their place was altered by adding a velocity $v_{fml}^{i,moa}(t+1)$ based on the subsequent formula:

$$y^i(t+1) = y^i(t) + v_{fml}^{i,moa}(t+1), \quad (7)$$

whereas $v_{fml}^i(t+1)$ has been defined utilizing the subsequent formula:

$$v_{fml}^{i,moa}(t+1) = \begin{cases} gv_{fml}^{i,moa}(t) + C_3 e^{-\beta r_{mf}^2} [x^{i,moa}(t) - y^i(t)] \\ \text{if male dominates female} \\ gv_{fml}^{i,moa}(t) + fl(t) \cdot r, \text{ otherwise} \end{cases} \quad (8)$$

In which $fl(t)$ refers to the random walk (RW) co-efficient, r_{mf} signifies the Cartesian distance amongst the male as well as female MFs, and C_3 represents the positive attraction constantly.

3.2.3. Mating of Mayflies

The crossover function was utilized from this technique for representing the mating procedure among 2 MFs and is utilized in the following: an optimum female crosses with an optimum male, the second-optimum female with a second-optimum male, etc. The outcomes attained afterwards these crosses were 2 offspring created based on the subsequent formulas:

$$offspring_1 = L \cdot male + (1 - L) \cdot female, \quad (9)$$

$$offspring_2 = L \cdot female + (1 - L) \cdot male, \quad (10)$$

In which *male* refers to the male parent, *female* signifies the female parent, and L denotes the arbitrary value in a specific interval. The primary velocity of offspring was set to 0.

3.2.4. Reduction of the Nuptial Dance and RW Coefficient

The nuptial dance executed by male MFs signified by co-efficient (t) and the RW applied by females depended on local searches depicted in Eqs. (6) and (8). However, arbitrary flights generate worse outcomes in arbitrary explorations. This issue takes place in the detail that the nuptial dance $d(t)$ or RW $fl(t)$ co-efficient generally considers tremendous primary values. It is mitigated by slowly decreasing the dance co-efficient $d(t)$ and RW co-efficient $fl(t)$ in all the iterations as demonstrated in the following formulas:

$$d(t) = d_0 \delta_d(t), \quad (11)$$

$$fl(t) = fl_0 \delta_{fl}(t), \quad (12)$$

In which, at all the iterations t of optimized problems, $\delta_d(t)$ and $\delta_{fl}(t)$ take set values from the interval of zero and one.

The fitness function of the MFO-FS technique is derived from maintaining a trade-off between the classification accuracy (maximum), and the number of selected features in every solution (minimum) attained by the chosen features, Eq. (13) defines the fitness function of the MFO-FS technique for evaluating the solutions as given below.

$$Fitness = \alpha \gamma_R(D) + \beta \frac{|R|}{|C|} \quad (13)$$

where $\gamma_R(D)$ signifies the classification error rate of a predefined classification model. $|R|$ indicates the cardinality of the chosen subset, and $|C|$ is the entire amount of features in the dataset, α , and β represent the parameters equivalent to the significance of classification quality and subset length.

3.3. Heart Disease Detection and Classification

Once the feature subsets are chosen, they are fed into the CNN-HNN model to carry out the classification process. CNN is a variant of ANN that includes distinctive layers as follows [19].

3.3.1. Convolution Layer

In this layer, the relationships between pixels of an image have been retained. It performs by learning their property. This process can be implemented by classifying the input image into small boxes of pixels. Generally, the mathematic operations can be considered as filter/kernel and image matrixes. The rectified linear unit (RLU) is the more commonly known activation function applied for the DL technique. ReLu function returns the input value when it is positive, and failing that, 0. It is formulated as follows:

$$ReLu(a) = \text{Max}(0, a) \quad (14)$$

3.3.2. Pooling Layer

This process is utilized for dropping redundant parameters is required. Spatial pooling decreases the dimension of the input dataset; however, it retains considerable attributes. It comprises:

- Max Pooling: this takes the most significant component from the feature maps.
- Average Pooling: Here, the abovementioned component is also taken into account.
- Sum Pooling: The sum of each component in the feature maps is used and calculated.

3.3.3. Fully Connected Layer

This layer converts the matrix into a vector. The feature map matrixes are transformed into (v_1, v_2, v_3, \dots) vector form and are fed into the neural network. The FC layers integrate the vector feature to form a model. At last, another activation function is employed for classification. The activation function utilized in CNN is generally softmax or sigmoid function. It is primarily utilized for dual classification. The more significant advantage of the activation function stems from its derivative being easier to determine. Based on the convention, the output value can be assumed with the interval of $[-1, 1]$. In this study, the HNN model is included in the final layer of the CNN to perform heart disease classification.

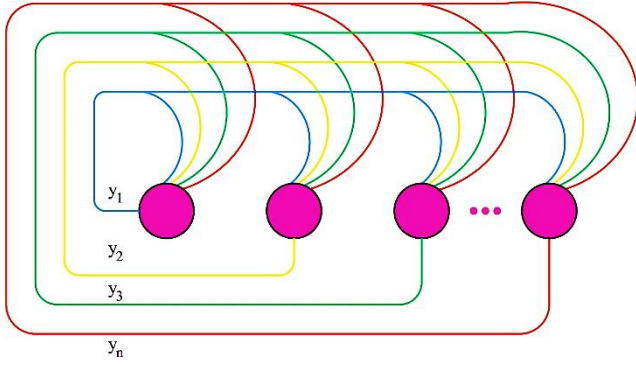


Fig. 2 Structure of HNN

The HNN comprises a group of N connected neurons that upgrade the activation value independently and asynchronously of another neuron [28]. Fig. 2 showcases the structure of HNN. A neuron i is described by their state $S_i = \pm 1$. The principle of HNN is to store binary patterns of the form $\{+1, -1\}^N$, and utilize a rule, named Hebb's rule, to learn them. In the inference state, the pattern is forecasted through a noisy input vector. Its robustness to noise is highly interesting in different types of applications. The "energy" of the Hopfield network is described as follows:

$$E = -\frac{1}{2} \sum_{i,j}^N S_i S_j w_{ij} \quad (15)$$

In Eq. (15), the weight associated with i and j neurons can be represented as w . The state of neuron i is denoted as S_i . The quantity is considered a Lyapunov function; it has remained stable or reduced once the network state is upgraded. Under repeated updating, the HNN converges to a local minimum in the energy function. Hence, the optimum value of the weight minimizes the energy function. Further, the theoretical storage capacity of HNN, from the assumption of the stability of each pattern, is determined by:

$$P_{\max} = \frac{N}{4 \ln N} \quad (16)$$

In Eq. (16), P_{\max} represents the maximal amount of unrelated patterns stored in N neuron recurrent network.

4. Results and Discussion

The experimental validation of the MFOFS-HML algorithm is tested under two benchmark datasets: The Cleveland dataset [21] and Framingham [22]. The first Cleveland dataset holds 13 attributes, and the MFO-FS model has chosen 8 attributes (age, chest, sex, serum_cholesterol, resting_blood_pressure, resting_electrocardiographic_results, maximum_heart_rate_achieved, and fasting_blood_sugar). Similarly, the Framingham dataset contains 15 attributes, and the MFO-FS model has elected 5 attributes (male, age, education, currentSmoker, and cigsPerDay).

Fig. 3 reports the convergence curve analysis of the MFO algorithm on the two datasets. The figures indicated that the MFO algorithm exhibits effective convergence over different iterations.

Fig. 4 provides a detailed result analysis of the MFOFS-HML technique on the test Cleveland dataset with 70% of training (TR) data and 20% of testing (TS) data. Fig. 4a indicates that the MFOFS-HML model has recognized 125 samples into the absence class and 104 samples into the presence class on 70% of TR data. Besides, Fig. 4b represents that the MFOFS-HML model has categorized 30 samples into the absence class and 29 samples into the presence class on 30% of TS data. Figs. 4c-4d demonstrates the precision-recall analysis of the MFOFS-HML approach under 70% of TR and 30% of TS data. The figures reported that the MFOFS-HML method had obtained maximum performance on the test dataset. Finally, Fig. 4e-4f illustrates the ROC investigation of the MFOFS-HML approach under 70% of TR and 30% of TS data. The figure specified that the MFOFS-HML method has correspondingly attained the highest ROC of 0.9957 and 0.9989 under absence and presence classes.

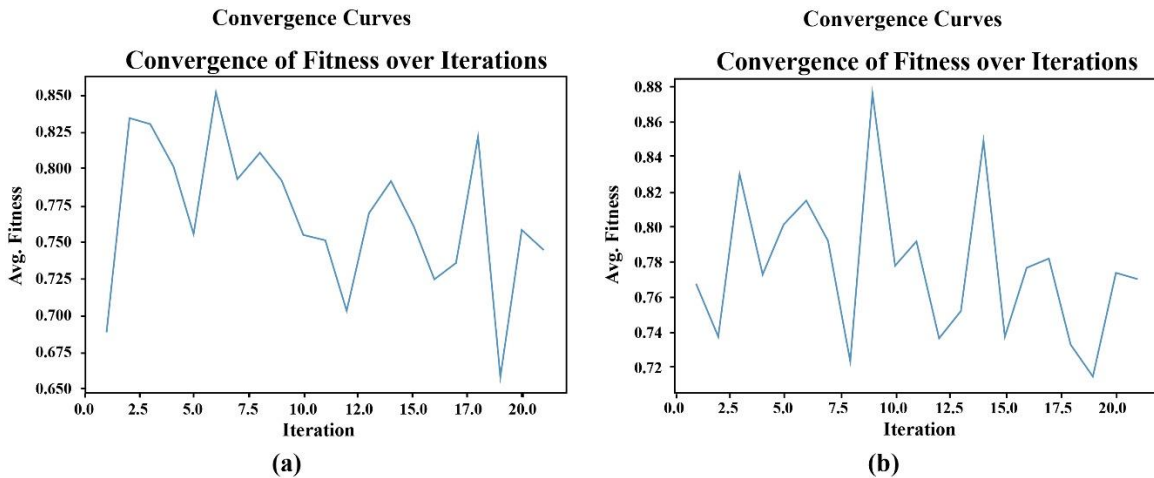


Fig. 3 a) Convergence Curves of Cleveland Dataset b) Convergence Curves of Framingham Dataset

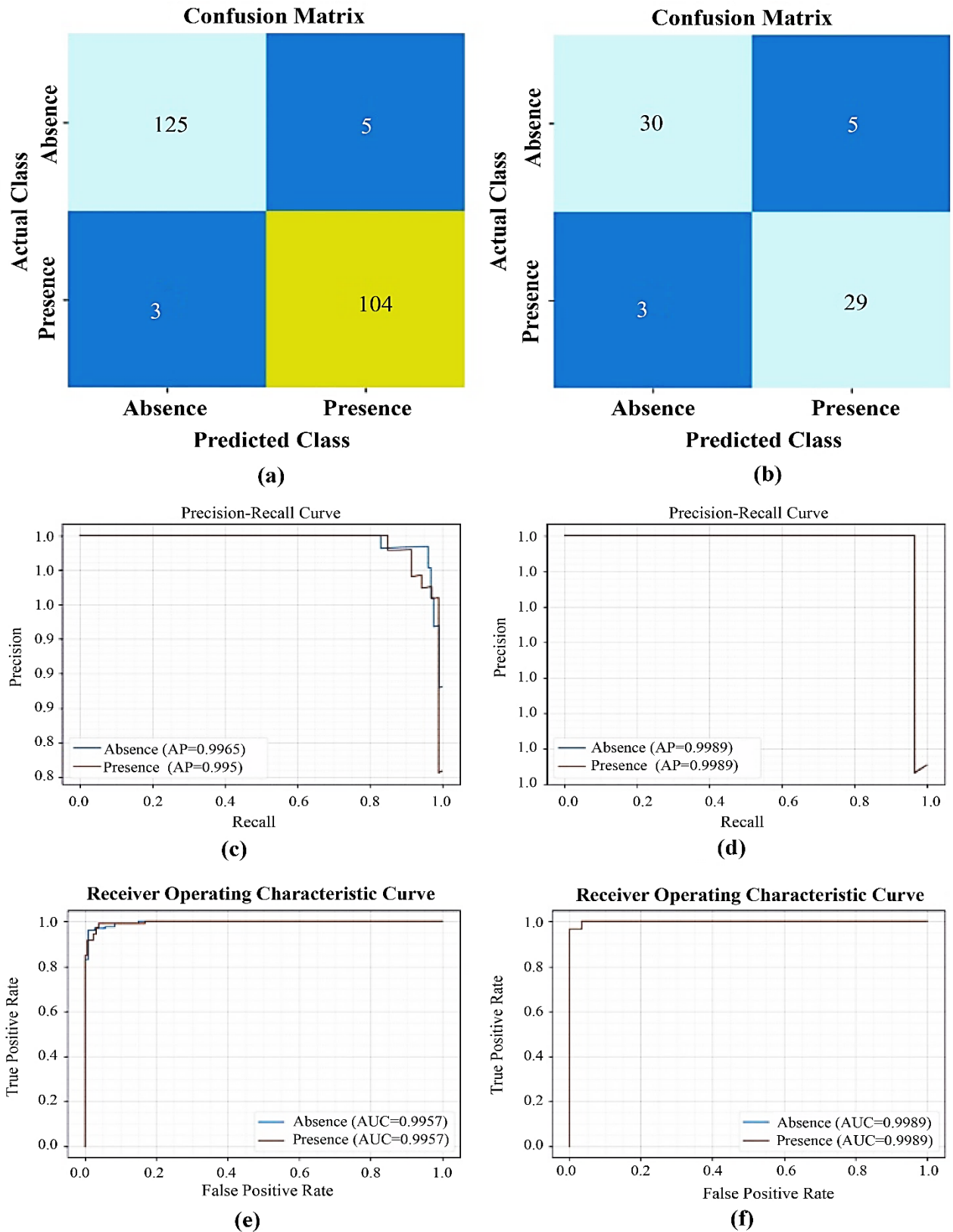
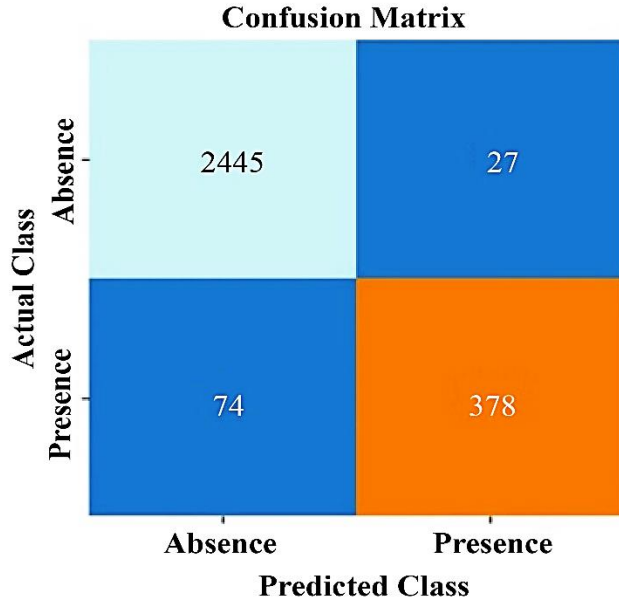
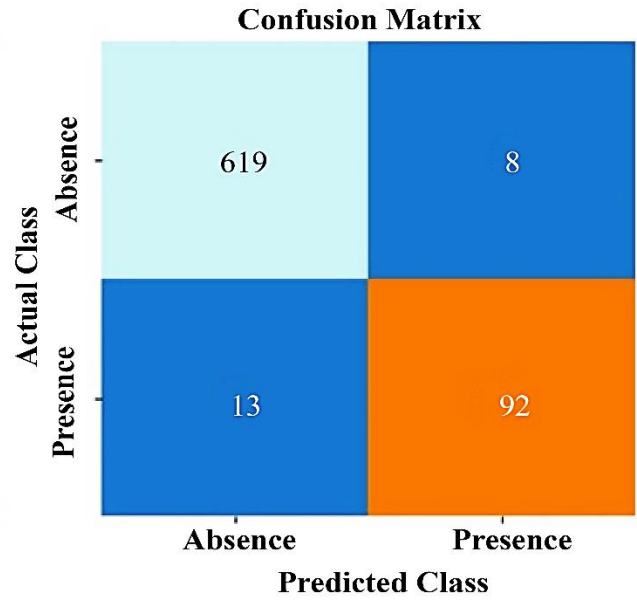


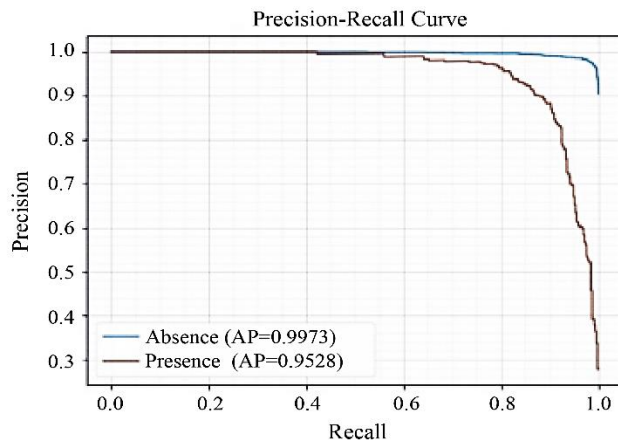
Fig. 4 Results of Cleveland Dataset Training Phase a) Confusion Matrix c) Precision-Recall Curve e) ROC Analysis / Testing Phase b) Confusion Matrix d) Precision-Recall Curve f) ROC Analysis /



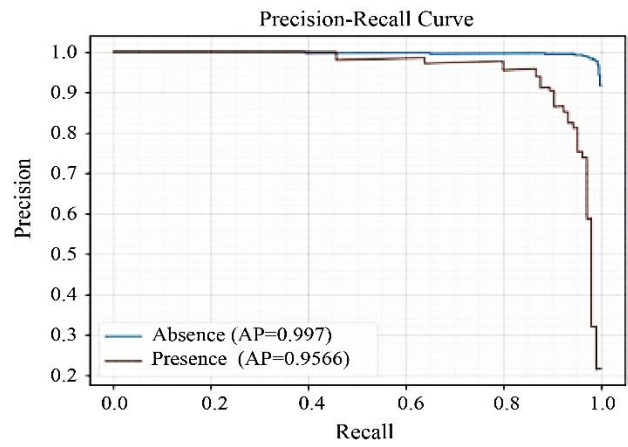
(a)



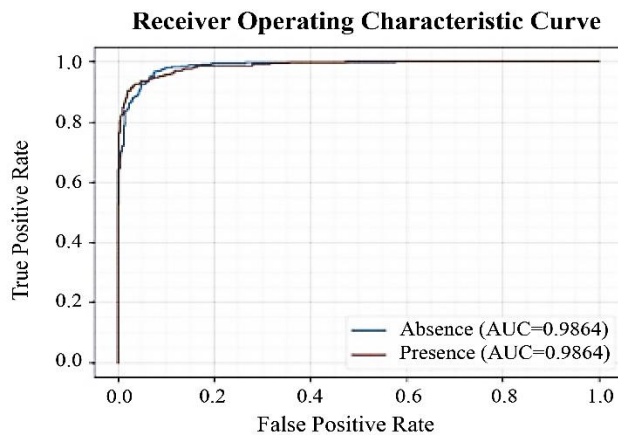
(b)



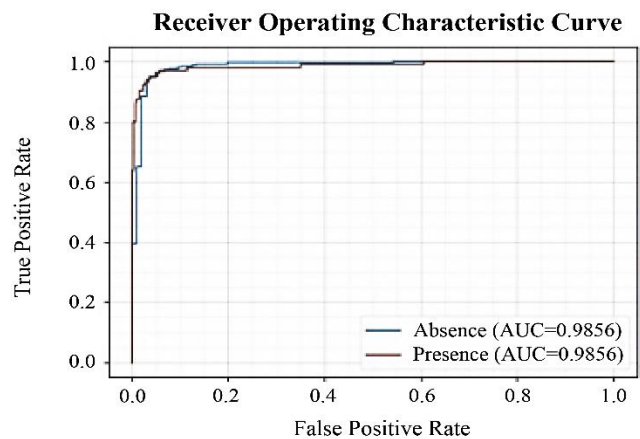
(c)



(d)

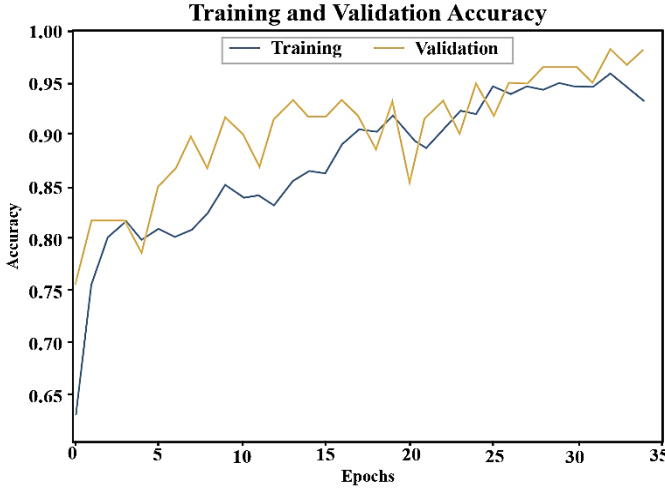


(e)

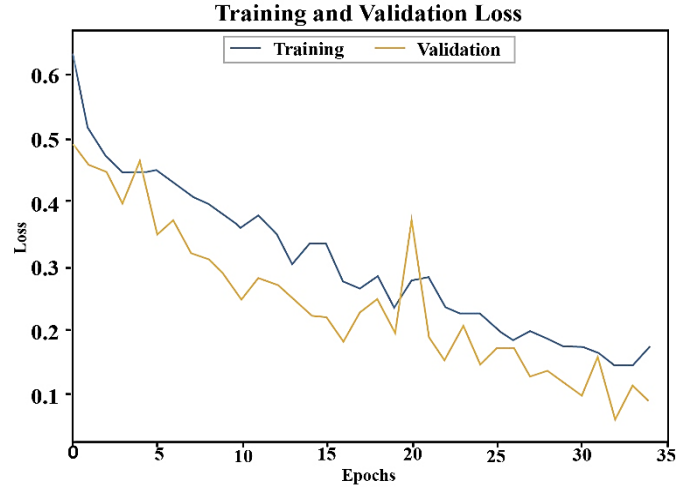


(f)

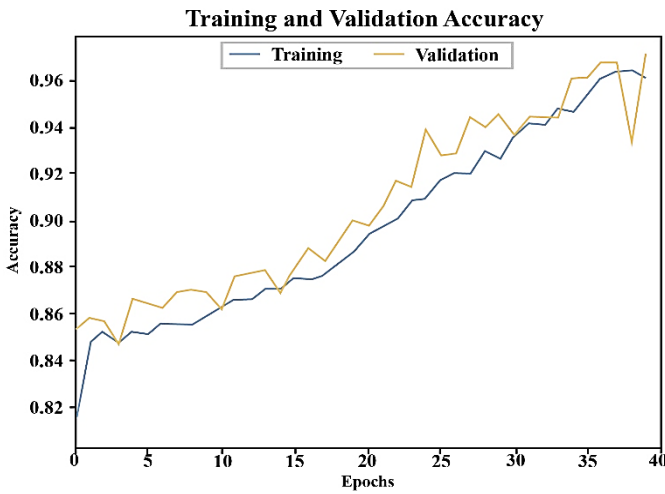
Fig. 5 Results of Framingham Dataset Training Phase a) Confusion Matrix c) Precision-Recall Curve e) ROC Analysis / Testing Phase b) Confusion Matrix d) Precision-Recall Curve f) ROC Analysis /



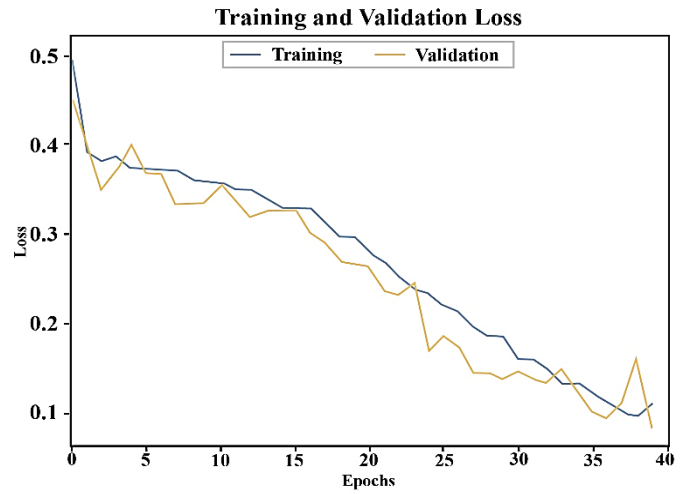
(a)



(b)



(c)



(d)

Fig. 6 (a and b) Graph of Accuracy and Loss- Cleveland Dataset (c and d) Graph of Accuracy and Loss-Framingham Dataset

Fig. 5 offers a detailed outcome analysis of the MFOFS-HML methodology on the test Framingham dataset with 70% of TR data and 20% of TS data. Fig. 5a depicts that the MFOFS-HML algorithm has recognized 2445 samples into the absence class and 378 samples into the presence class on 70% of TR data. Also, Fig. 5b represents that the MFOFS-HML model has categorized 619 samples into absence class and 92 samples into presence class on 30% of TS data. Figs. 5c-5d illustrates the precision-recall analysis of the MFOFS-HML technique under 70% of TR and 30% of TS data. The figures reported that the MFOFS-HML approach had obtained maximal performance on the test dataset. At last, Fig. 5e-5f demonstrates the ROC examination of the MFOFS-HML approach under 70% of TR and 30% of TS data. The figure represented that the MFOFS-HML methodology has obtained superior ROC of 0.9864 and 0.9856 under absence and presence classes correspondingly.

Fig. 6 depicts the accuracy and loss graph analysis of the MFOFS-HML algorithm on the two datasets. The outcome outperforms that the accuracy value tends to enhance, and the loss value tends to decrease with an increasing epoch count. It has been demonstrated that validation accuracy is higher, and the training loss is lower on the two datasets.

Table 1 reports an overall result analysis of the MFOFS-HML model and CNN-HNN model on the two applied datasets. On the Cleveland training dataset, the CNN-HNN model has attained $accu_y$ of 93.25%, $prec_n$ of 94.02%, $recal_l$ of 92.69%, $F1_{score}$ of 93.10% and a ROC-AUC score of 98.79%. Similarly, on the Cleveland training dataset, the MFOFS-HML model has reported $accu_y$ of 96.62%, $prec_n$ of 96.53%, $recal_l$ of 96.68%, $F1_{score}$ of 96.60% and a ROC-AUC score of 99.57%. Also, on the Framingham training dataset, the CNN-HNN approach has reached $accu_y$ of 93.91%, $prec_n$ of 95.25%, $recal_l$ of 81.12%, $F1_{score}$ of

86.29% and a ROC-AUC score of 96.95%. Eventually, on the Framingham training dataset, the MFOFS-HML technique has reported $accu_y$ of 96.55%, $prec_n$ of 95.20%, $reca_l$ of 91.27%, $F1_{score}$ of 93.10% and a ROC-AUC score of 98.64%.

In order to demonstrate the enhanced performance of the MFOFS-HML methodology, a detailed comparison study is made in Table 2 [23-25]. Fig. 7 illustrates a brief $accu_y$ inspection of the MFOFS-HML with current approaches. The figure implied that the CFS-Naïve Bayes, CFS-Logistic Regression, and CFS-JRip models had shown the least $accu_y$ value of 84.15%, 83.17%, and 74.26% respectively. At the same time, the GB, XGBoost, AdaBoost, and SGDC algorithms have gained somewhat highest $accu_y$ values of 90.39%, 91.89%, 91.88%, and 92.14% correspondingly.

Table 1. Result analysis of MFOFS-HML and CNN-HNN techniques on two datasets

Metrics	CNN-HNN		MFOFS-HML	
	Training	Testing	Training	Testing
Cleveland Dataset				
Accuracy	93.25	95.00	96.62	98.33
Precision	94.02	95.05	96.53	98.39
Recall	92.69	95.00	96.68	98.33
F1-Score	93.10	95.00	96.60	98.33
ROC-AUC Score	98.79	98.89	99.57	99.89
Framingham Dataset				
Accuracy	93.91	94.54	96.55	97.13
Precision	95.25	93.51	95.20	94.97
Recall	81.12	83.33	91.27	93.17
F1-Score	86.29	87.45	93.10	94.04
ROC-AUC Score	96.95	97.13	98.64	98.56

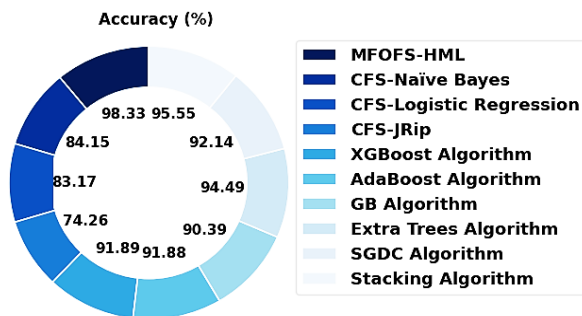


Fig. 7 $Accu_y$ analysis of the MFOFS-HML technique with exiting methodologies

Along with that, the Extra Trees and Stacking models have reached reasonably closer $accu_y$ of 94.49% and 95.55%, respectively. However, the MFOFS-HML model has shown better performance with higher $accu_y$ of 98.33%.

Fig. 8 depicts a detailed $prec_n$ examination of the MFOFS-HML with existing approaches. The figure revealed that the CFS-Naïve Bayes, CFS-Logistic Regression, and CFS-JRip models have shown minimal $prec_n$ value of 84.30%, 83.20%, and 74.10% respectively. Concurrently, the GB, XGBoost, AdaBoost, and SGDC models have reached somewhat improved $prec_n$ values of 90.43%, 92.21%, 90.97%, and 93.38% correspondingly. Followed by the Extra Trees and Stacking models have reached reasonably closer $prec_n$ of 94.21% and 96.8%, correspondingly. But, the MFOFS-HML system has demonstrated better performance with higher $prec_n$ of 98.39%.

Table 2. Comparative analysis of MFOFS-HML technique with existing methods

Methods	$Accu_y$	$Prec_n$	$Reca_l$	$F1_{score}$
MFOFS-HML	98.33	98.39	98.33	98.33
CFS-Naïve Bayes	84.15	84.30	84.20	84.10
CFS-Logistic Regression	83.17	83.20	83.20	83.10
CFS-JRip	74.26	74.10	74.30	74.10
XGBoost Algorithm	91.89	92.21	92.96	92.78
AdaBoost Algorithm	91.88	90.97	93.04	92.01
GB Algorithm	90.39	90.43	90.93	90.21
Extra Trees Algorithm	94.49	94.21	94.32	94.66
SGDC Algorithm	92.14	93.38	91.87	92.59
Stacking Algorithm	95.55	96.80	95.32	95.74

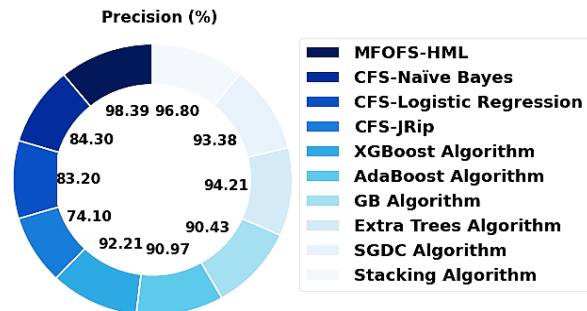


Fig. 8 $Prec_n$ analysis of the MFOFS-HML technique with exiting methodologies

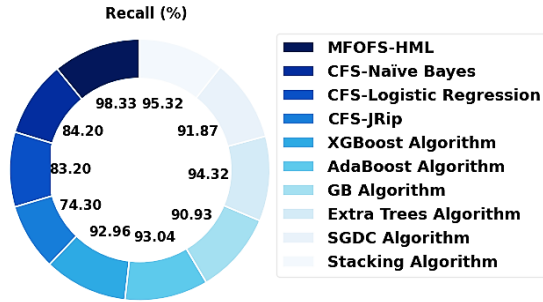


Fig. 9 $Recall_i$ analysis of the MFOFS-HML technique with exiting methodologies

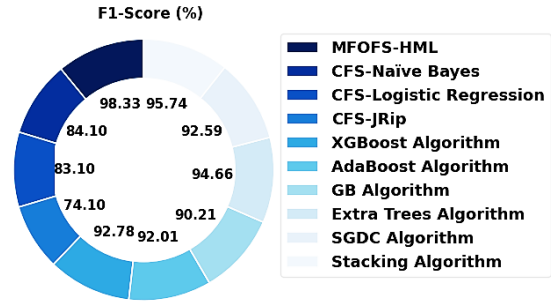


Fig. 10 $F1_{score}$ analysis of the MFOFS-HML technique with exiting methodologies

Fig. 9 demonstrates a brief $recall_i$ analysis of the MFOFS-HML with existing approaches. The figure implied that the CFS-Naïve Bayes, CFS-Logistic Regression, and CFS-JRip models had outperformed lesser $recall_i$ value of 84.20%, 83.20%, and 74.30% respectively. Simultaneously, the GB, XGBoost, AdaBoost, and SGDC models have gained slightly higher $recall_i$ values of 90.93%, 92.96%, 93.04%, and 91.87% correspondingly. Besides, the Extra Trees and Stacking systems have reached reasonably closer $recall_i$ of 94.32% and 95.32%, correspondingly. At last, the MFOFS-HML approach has exhibited better performance with superior $recall_i$ of 98.33%.

Fig. 10 showcases a brief $F1_{score}$ investigation of the MFOFS-HML with existing approaches. The figure exposed that the CFS-Naïve Bayes, CFS-Logistic Regression, and CFS-JRip models have shown worse $F1_{score}$ value of 84.10%, 83.10%, and 74.10% respectively. Likewise, the GB, XGBoost, AdaBoost, and SGDC models have attained somewhat maximal $F1_{score}$ values of 90.21%, 92.78%, 92.01%, and 92.59% correspondingly. In addition, the Extra Trees and Stacking methodologies have gained reasonably closer $F1_{score}$ of 94.66% and 95.74% correspondingly. Lastly, the MFOFS-HML approach has portrayed optimum performance with increased $F1_{score}$ of 98.33%.

These results and discussion show that the MFOFS-HML algorithm has accomplished superior performance over other models due to the inclusion of the MFOFS technique and CNN-HNN model.

5. Conclusion

This study presented a new MFOFS-HML approach to detect and classify heart diseases. The proposed MFOFS-HML model involves three major processes: data pre-processing, MFO-FS-based feature subset selection, and CNN-HNN classification. Initially, the presented MFOFS-HML model applies data pre-processing to transform the actual data into a useful format. Followed by the MFOFS technique is used for the effective selection of features from the pre-processed data. At last, the CNN-HNN model is employed for the detection and classification process. The experimental validation of the MFOFS-HML model is tested using two benchmark datasets, Cleveland and Framingham datasets. A brief comparison study reported the enhanced outcomes of the presented MFOFS-HML model over recent approaches. Therefore, the MFOFS-HML model can be applied for effectual heart disease detection and classification. In future, the hyperparameter tuning strategy can be incorporated into the MFOFS-HML model to improve the classification performance.

References

- [1] Tougui, I., Jilbab, A., and El Mhamdi, J, "Heart Disease Classification Using Data Mining Tools and Machine Learning Techniques," *Health and Technology*, vol. 10, no. 5, pp.1137-1144, 2020. *Crossref*, <https://doi.org/10.1007/s12553-020-00438-1>
- [2] Shuangquan Li et al., "Health Checkup Could Reveal Chronic Disorders with Support from Artificial Intelligence," *International Journal of Engineering Trends and Technology*, vol. 67, no. 11, pp. 8-15. *Crossref*, [10.14445/22315381/IJETT-V67I11P202](https://doi.org/10.14445/22315381/IJETT-V67I11P202)
- [3] Dilmurod Nabiev, and Khayit Turaev, "Study of Synthesis and Pigment Characteristics of the Composition of Copper Phthalocyanine with Terephthalic Acid," *International Journal of Engineering Trends and Technology*, vol. 70, no. 8, pp. 1-9, 2022. *Crossref*, <https://doi.org/10.14445/22315381/IJETT-V70I8P201>
- [4] Shwetambari Borade et al., "Deep Scattering Convolutional Network for Cosmetic Skin Classification," *International Journal of Engineering Trends and Technology*, vol. 70, no. 7, pp. 10-23, 2022. *Crossref*, <https://doi.org/10.14445/22315381/IJETT-V70I7P202>
- [5] Vaibhav Gupta, and Dr.Pallavi Murghai Goel, "Heart Disease Prediction Using ML," *SSRG International Journal of Computer Science and Engineering*, vol. 7, no. 6, pp. 17-19, 2020. *Crossref*, <https://doi.org/10.14445/23488387/IJCSE-V7I6P105>
- [6] Ibrahim M. El-Hasnony et al., "Multi-Label Active Learning-Based Machine Learning Model for Heart Disease Prediction," *Sensors*, vol. 22, no. 3, p. 1184, 2022. *Crossref*, <https://doi.org/10.3390/s22031184>

- [7] Ahsan, M.M., and Siddique, Z, "Machine Learning-Based Heart Disease Diagnosis: A Systematic Literature Review," *Artificial Intelligence in Medicine*, vol. 128, p.102289, 2022. *Crossref*, <https://doi.org/10.1016/j.artmed.2022.102289>
- [8] Divya Sharma et al., "Machine Learning Approach to Classify Cardiovascular Disease in Patients with Nonalcoholic Fatty Liver Disease in the UK Biobank Cohort," *Journal of the American Heart Association*, vol. 11, no. 1, p. E022576, *Crossref*, <https://doi.org/10.1161/jaha.121.022576>
- [9] Khalid Mahmood Aamir et al., "Automatic Heart Disease Detection by Classification of Ventricular Arrhythmias on ECG Using Machine Learning," *Computers, Materials & Continua*, vol. 71, no. 1, pp.17-33. *Crossref*, <http://dx.doi.org/10.32604/cmc.2022.018613>
- [10] Md Mamun Ali et al., "Heart Disease Prediction Using Supervised Machine Learning Algorithms: Performance Analysis and Comparison," *Computers in Biology and Medicine*, vol.136, P. 104672, 2021. *Crossref*, <https://doi.org/10.1016/j.compbiomed.2021.104672>
- [11] Khourdifi, Y., and Bahaj, M, "Heart Disease Prediction and Classification Using Machine Learning Algorithms Optimized by Particle Swarm Optimization and Ant Colony Optimization," *International Journal of Intelligent Engineering and Systems*, vol. 12, no.1, pp. 242-252, 2019. *Crossref*, <http://dx.doi.org/10.22266/ijies2019.0228.24>
- [12] Rajkumar Gangappa Nadakinamani, "Clinical Data Analysis for Prediction of Cardiovascular Disease Using Machine Learning Techniques," *Computational Intelligence and Neuroscience*, 2022. *Crossref*, <https://doi.org/10.1155/2022/2973324>
- [13] Suresh, T. et al., "A Hybrid Approach To Medical Decision-Making: Diagnosis of Heart Disease with Machine-Learning Model," *International Journal of Electrical & Computer Engineering*, vol. 12, no. 2, pp. 1831-1838, 2022. *Crossref*, <http://dx.doi.org/10.11591/ijece.v12i2.pp1831-1838>
- [14] Nandakumar Pandiyan, and Subhashini Narayan, "Prediction of Cardiac Disease Using Kernel Extreme Learning Machine Model," *International Journal of Engineering Trends and Technology*, vol. 70, no. 11, pp. 364-377, 2022. *Crossref*, <https://doi.org/10.14445/22315381/IJETT-V70I11P238>
- [15] M. Kavitha et al., "Heart Disease Prediction Using Hybrid Machine Learning Model," *2021 6th International Conference on Inventive Computation Technologies (ICICT)*, pp. 1329-1333, 2021. *Crossref*, <https://doi.org/10.1109/ICICT50816.2021.9358597>
- [16] Khemphila, A, and Boonjing, V, "Heart Disease Classification Using Neural Network and Feature Selection," *2011 21st International Conference on Systems Engineering, IEEE*, pp. 406-409, 2011.
- [17] K. Zervoudakis, and S. Tsafarakis, "A Mayfly Optimization Algorithm," *Computers & Industrial Engineering*, vol. 145, p. 106559, 2020. *Crossref*, <https://doi.org/10.1016/j.cie.2020.106559>
- [18] Luis Fabiano Barone Martins et al., "Mayfly Optimization Algorithm Applied to the Design of PSS and SSSC-POD Controllers for Damping Low-Frequency Oscillations in Power Systems," *International Transactions on Electrical Energy Systems*, vol. 2022, pp. 1-23, 2022. *Crossref*, <https://doi.org/10.1155/2022/5612334>
- [19] Dai Quoc Nguyen et al., "A Novel Embedding Model for Knowledge Base Completion Based on Convolutional Neural Network," *Proceedings of the 2018 Conference of the North American Chapter of the Association for Computational Linguistics: Human Language Technologies*, vol. 2, 2018.
- [20] I.Lakshmi, "Prediction Analysis on Heart Disease Using HNB and NB Techniques," *SSRG International Journal of Computer Science and Engineering*, vol. 5, no. 10, pp. 11-15, 2018. *Crossref*, <https://doi.org/10.14445/23488387/IJCSE-V5I10P105>
- [21] [Online]. Available: <https://www.kaggle.com/datasets/naveengowda16/logistic-regression-heart-disease-prediction>
- [22] [Online]. Available: <https://www.kaggle.com/datasets/sulianova/cardiovascular-disease-dataset>
- [23] Louridi, N. et al., "Machine Learning-Based Identification of Patients with a Cardiovascular Defect," *Journal of Big Data*, vol. 8, 2021. *Crossref*, <https://doi.org/10.1186/s40537-021-00524-9>
- [24] Karna Vishnu Vardhana Reddy et al., "Heart Disease Risk Prediction Using Machine Learning Classifiers with Attribute Evaluators," *Applied Sciences*, vol. 11, no. 18, P.8352, 2021. *Crossref*, <https://doi.org/10.3390/app11188352>
- [25] S. Sivasubramaniam, and S. P. Balamurugan, "An Optimal Artificial Neural Network Based Heart Disease Classification Model," *Turkish Journal of Physiotherapy and Rehabilitation*, vol. 32, no. 3,
- [26] Ramalingam, V.V, Dandapath, A., and Raja, M.K, "Heart Disease Prediction Using Machine Learning Techniques: A Survey," *International Journal of Engineering & Technology*, vol. 7, no. 2.8, pp.684-687, 2018. *Crossref*, <http://dx.doi.org/10.14419/ijet.v7i2.8.10557>
- [27] Pengpai Li et al., "Prediction of Cardiovascular Diseases by Integrating Multi-Modal Features with Machine Learning Methods," *Biomedical Signal Processing and Control*, vol. 66, P.102474, 2021. *Crossref*, <https://doi.org/10.1016/j.bspc.2021.102474>
- [28] Bocheng Bao et al., "Dynamical Effects of Neuron Activation Gradient on Hopfield Neural Network: Numerical Analyses and Hardware Experiments," *International Journal of Bifurcation and Chaos*, vol. 29, no. 4, p.1930010, 2019. *Crossref*, <https://doi.org/10.1142/S0218127419300106>